

Determination of Droplet Shape in Digital Microfluidic Systems Using Two-Dimensional Flow Analysis

A. Ahmadi*, H. Najjaran*, J. F. Holzman*, and M. Hoorfar*

*School of Engineering, University of British Columbia, mina.hoorfar@ubc.ca

ABSTRACT

The steady-state motion of microdroplets in the electrowetting-based digital microfluidic systems is modeled. Kinematics of fluid flow inside and around the microdroplet is numerically calculated. It is found that the effects of the vertical velocity component especially near the receding and advancing faces plays a crucial role in predicting the microdroplet dynamics. Moreover, it is shown that fluid flow kinematics is important in determining the microdroplet shape.

Keywords: digital microfluidic, electrowetting, microdroplet, lab-on-a-chip, dynamics, hysteresis

1 INTRODUCTION

Digital microfluidic systems which are based on the motion of discrete microdroplets on a patterned substrate are new generations of lab-on-a-chip devices. Electrowetting phenomena have been used as one of the most successful methods to actuate the microdroplets on the arrays of electrodes of microfluidic devices [1-3]. Such devices have shown a high level of scalability and reconfigurability. Most recent work has focused on fabricating [1-3] and presenting new applications for digital microfluidic systems [4]. Modeling and simulation of digital microfluidic systems are another crucial aspect in the design and optimization processes for real-time control of the microdroplets. An accurate model of the system allows for predicting of the device performance before going through the fabrication process. Such a model must be capable of predicting motion of the microdroplet which is a function of surface, microdroplet solution and filler properties as well as the structure of the system [1]. Several forces such as actuation force, shear force, contact line force and filler force are acting on the microdroplet and numerous effects such as hysteresis have to be considered. Thus, the development of an inclusive model for digital microfluidic systems is not a trivial task. This paper focuses on modeling the dynamics of microdroplet motion in these electrowetting-based digital microfluidic systems.

In the simplest case, the Poiseuille flow assumption has been used to model dynamics (effects of different forces) of microdroplet motion [5-7]. This assumption is based on a one-dimensional flow and pressure distribution inside the microdroplet. Such one-dimensional flow models are easy to implement, though they overestimate the microdroplet transport velocity. Moreover, since it is ignoring the

pressure gradient across the microdroplet, the predicted microdroplet shape is independent of the microdroplet aspect ratio. It has been shown that a two-dimensional analysis is needed for accurate modeling of the microdroplet dynamics in digital microfluidic systems [8]. In this work, a computational two-dimensional approach for modeling microdroplet “motion” in an electrowetting-based digital microfluidic system is introduced. The result of the new approach is compared to the experimental and one-dimensional results, and it is shown that the proposed two-dimensional approach provides a more realistic approximation of the microdroplet transport velocity as a function of applied voltage. Finally, fluid flow kinematics is used to predict the microdroplet shape and contact angle.

2 FORCE ANALYSIS

Numerous phenomena affect the dynamics of the microdroplet motion in electrowetting-based digital microfluidic systems. Applied voltages cause the actuating force in such devices, while hysteresis phenomena and resisting forces lead to a threshold voltage and impeded microdroplet motion. To accurately model such a system, it is important to include all of these effects. Properties of the filler fluid (which is used in closed digital microfluidic devices), surface adsorption and contact line friction are all important phenomena, as kinematics of fluid inside and outside of the microdroplet has a crucial effect on microdroplet motion. All these effects are introduced and formulated in this section.

2.1 Actuating Force

Applying voltage to the electrodes underlying the microdroplet causes the actuating force for moving the microdroplet in electrowetting-based digital microfluidic systems. This force acts along the triple line which is given by

$$F_{act} = \frac{C_e}{2} V^2, \quad (1)$$

where e is the distance between two ends of the triple line normal to the direction of the motion and V is the applied voltage. The structural capacitance per unit area, C , is defined as

$$C = \frac{\epsilon_0}{\sum_i d_i / \epsilon_i} \quad (2)$$

The total capacitance is defined as a composition of multiple capacitance layers, where the i^{th} layer in the structure has a thickness, d_i , a dielectric constant, ϵ_i , and ϵ_0 is the permittivity of free-space. The schematic of such a structure is shown in figure 1.

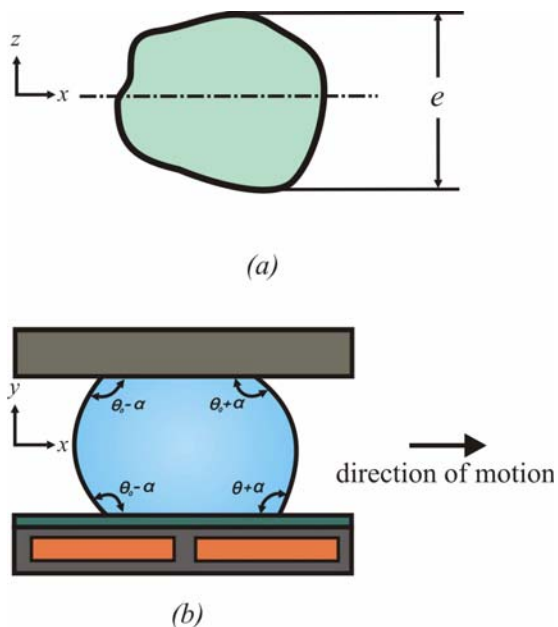


Figure 1: (a) The distance between two ends of the triple line normal to the direction of the motion. (b) Schematic of the microdroplet at the onset of actuation, where θ_0 is the nonactuated contact angle, θ is the actuated contact angle and α denotes the change in contact angle due to hysteresis effects.

2.2 Hysteresis Effect

In the electrowetting-based digital microfluidic systems there exists a threshold voltage below which microdroplet motion cannot occur. This is due to the fact that no surface is ideal and morphological and chemical defects exist. Analyses of these threshold voltage conditions have been introduced before for open systems [9]. In this paper, the threshold voltage is calculated for a closed electrowetting-based digital microfluidic system. Using a force balance analysis for the geometry shown in figure 1.b, it can be shown that the actuated contact angle at the threshold voltage, $\theta(V_{tr})$, can be expressed as

$$\theta(V_{tr}) = \cos^{-1}[2\cos(\theta_0 - \alpha) - \cos(\theta_0 + \alpha)] - \alpha \quad (3)$$

Using the Lippmann-Young Law this threshold condition can be expressed as

$$V_{tr} = \sqrt{\frac{2\gamma}{C} \{\cos[\theta(V_{tr})] - \cos(\theta_0)\}} \quad (4)$$

As a result, the actuation force from equation (1) can be rewritten as

$$F_{act} = \frac{Ce}{2} (V^2 - V_{tr}^2), \quad (5)$$

where the added term represents the decrease in the actuation force once transport is initiated.

2.3 Contact Line Force

To include the effects of molecular displacement around the contact line [10], it is necessary to include within our model a contact line friction force. This friction force is linearly dependent on the transport velocity of the microdroplet at low velocities [11] and can be quantified as

$$F_{cl} = 4\pi r \xi u, \quad (6)$$

where u is the transport velocity of the microdroplet, r is the radius of the microdroplet and $\xi = 0.04$ is the friction factor obtained empirically in [11].

2.4 Filler Effects

Filler effects in a closed digital microfluidic system are highly complex phenomena. These effects are calculated here using COMSOL Multiphysics software. The software uses a finite element method (FEM) with the adaptive mesh shown in figure 2 and models the drag force on the microdroplet (being proportional to the velocity gradients at the microdroplet surface). To improve the accuracy of the FEM solution a pair of weak-constraint variables is used to enforce the no-slip condition on the microdroplet.

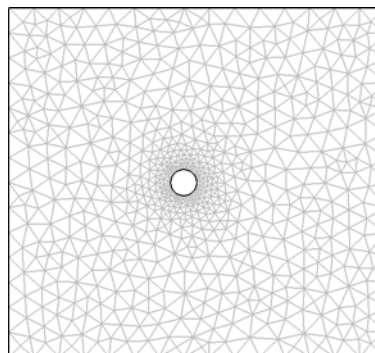


Figure 2: FEM mesh used in COMSOL multiphysics.

2.5 Shear Force

The Poiseuille flow assumption has been used to model the kinematics of fluid flow inside microdroplets, though it overestimates the transport velocity of the microdroplet. This discrepancy arises from the assumed constant velocity profile along the microdroplet, leading to constant shear stress. As shown here, the true fluid flow kinematics (especially near the advancing and receding faces) significantly deviates from this one-dimensional behavior. Indeed, the three-dimensional nature of the flow inside the microdroplet leads to larger shear stress estimation near the receding and advancing faces. A pseudo-three-dimensional approach is proposed here to solve the governing equations inside the microdroplet and to find a more realistic approximation for shear stress distribution along the microdroplet. In this analysis, the solution of the fluid flow kinematics in the meridian plane (x-y plane) is extended to a collection of parallel planes. Summing of all the planar shear forces along the microdroplet walls gives the total shear force as

$$F_w = 2 \sum_{k=1}^m \sum_{i=1}^n \mu_{md} \left. \frac{du}{dy} \right|_{ik} dA_{ik}, \quad (7)$$

where dA_{ik} is the area element in the x-z plane which is in contact with the top (or bottom) wall, and $\mu_{md} \left. \frac{du}{dy} \right|_{ik}$ is the shear stress at the area element (see figure 3).

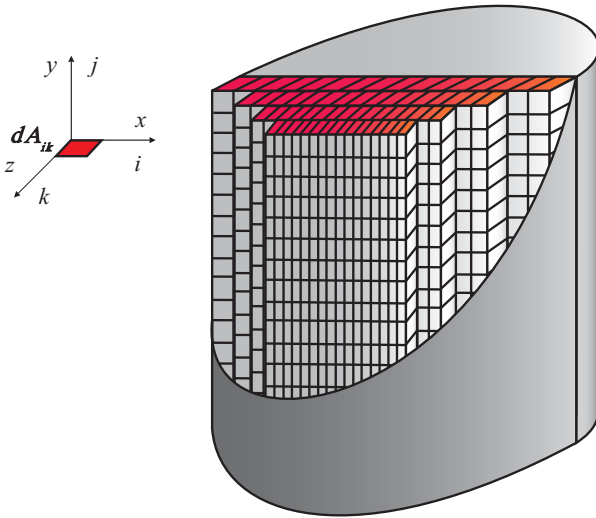


Figure 3: Discretization of the microdroplet for calculating shear force is shown.

2.6 Force Balance

The steady-state condition of the microdroplet motion (under which a constant transport velocity is assumed) is considered here by way of a force balance equation. The actuating force and resisting forces are described by the condition

$$F_{act} = F_{cl} + F_{drag} + F_w. \quad (8)$$

The actuation force (F_{act}) is a function of the applied voltage. In contrast to this, the contact line force (F_{cl}) is an explicit function of the transport velocity, while the drag force (F_{drag}) and shear force (F_w) are implicit functions of the transport velocity. An iterative method is used to solve equation (8) and find the transport velocity of the microdroplet as a function of applied voltage. This iterative method is presented in the next section.

3 COMPUTATIONAL APPROACH

The numerical algorithm used to solve equation (8) is shown in figure 4. By solving the governing equations inside the microdroplet, the internal pressure distribution is obtained. The Laplace equation is used to find the shape (curvature) of the advancing and receding faces as this equation correlates the internal and external pressure differences to the principle curvatures ($\frac{1}{r}$ and $\frac{1}{r_m}$). The relationship becomes

$$\Delta P = \gamma \left(\frac{1}{r} + \frac{1}{r_m} \right). \quad (9)$$

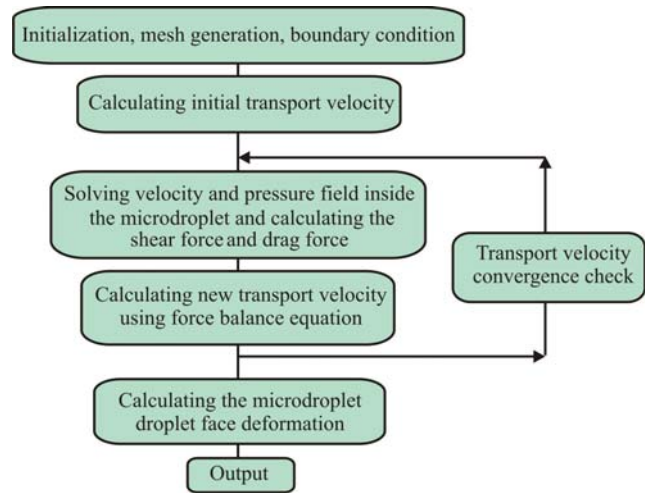


Figure 4: The iterative method implemented to solve the force balance in equation (8).

Knowing the left hand side of equation (9) for each point on the boundary gives the curvature of the surface, r_m . This is in contrast to one-dimensional models for which this curvature must be assumed to be constant.

4 RESULTS

The system introduced by Pollack et al. [1] is modeled here to verify the two-dimensional approach, and the results of this two-dimensional analysis are compared to these experimental results in figure 5. One-dimensional results are also included for a comparison. It is readily apparent from this figure that the one-dimensional analysis, which neglects the shear stress caused by the vertical component of the velocity, can be improved with the two-dimensional model. The two-dimensional analysis and computational approach gives a more realistic approximation of the true microdroplet transport velocity. Interestingly, the proposed model also allows for a more accurate representation of the microdroplet curvature. The results of such an analysis are shown in figure 6.

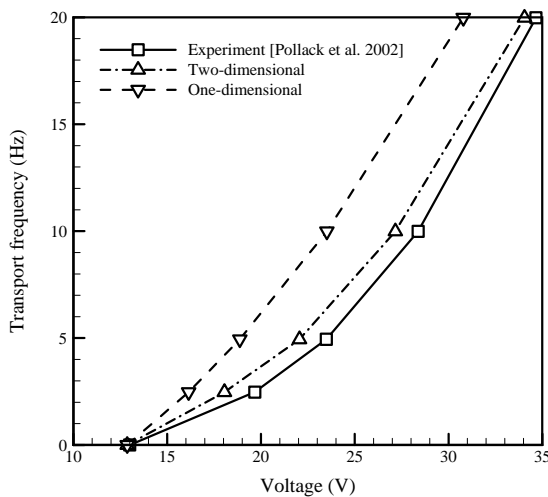


Figure 5: Transport frequency of the microdroplet for different voltages.

5 CONCLUSION

Motion of microdroplets in electrowetting-based digital microfluidic systems is modeled. The effect of the fluid flow kinematics on microdroplet motion is investigated, and it is shown that an accurate understanding of the motion requires multi-dimensional analyses. Such approaches can successfully predict the internal dynamics and shape of microdroplets within existing digital microfluidic systems.

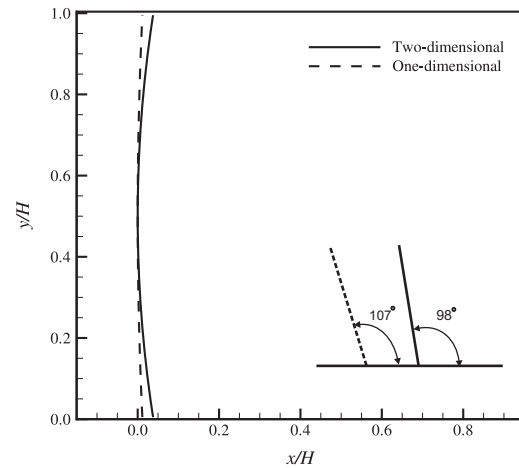


Figure 6: Shape of the microdroplet face obtained from two approaches.

REFERENCES

- [1] M. G. Pollack, R. B. Fair and A. D. Shenderov, *Appl. Phys. Lett.* 77, 1725, 2000.
- [2] J. Lee, H. Moon, J. Fowler, C. J. Kim and T. Schoellhammer, *Proc. IEEE Int. Conf. MEMS*, 499, 2001.
- [3] M. Abdelgawad, A. R. Wheeler, *Adv. Mater.* 19, 133, 2007.
- [4] R. B. Fair, A. Khlystov, T. D. Taylor, V. Ivanov, R. D. Evans, V. Srinivasan, V. K. Pamula, M. G. Pollack, P. B. Griffin and J. Zhou, *IEEE Des. Test Comput.* 10, 2007.
- [5] E. S. Baird, K. Mohseni, *Nanoscale Microscale Thermophys. Eng.* 11, 109, 2007.
- [6] V. Bahadur, S. V. Garimella, *J. Micromech. Microengineering* 16, 1494, 2006.
- [7] S. W. Walker, B. Shapiro, *J. Microelectromech. Syst.* 15, 986, 2006.
- [8] A. Ahmadi, H. Najjaran, J. F. Holzman and M. Hoorfar, *Proc. Nanotech*, 561, 2008.
- [9] J. Berthier, P. Dubois, P. Clementz, P. Claustre, C. Peponnet and Y. Fouillet, *Sens. Actuators A* 134, 471, 2007.
- [10] T. Blake, J. De Coninck, *Adv. Colloid Interface Sci.* 96, 21, 2002.
- [11] H. Ren, R. B. Fair, M. G. Pollack and E. J. Shaughnessy, *Sens. Actuators B* 87, 201, 2002.